New Phytologist

Methods

New tools for labeling silica in living diatoms

Julien Desclés[1], Mathieu Vartanian[1], Abdeslam El Harrak[2], Michelle Quinet[1], Nicolas Bremond[2], Guillaume Sapriel[1], Jérome Bibette[2] and Pascal J. Lopez[1]

[1]Laboratoire Biologie Moléculaire des Organismes Photosynthétiques CNRS UMR-8186, Ecole Normale Supérieure, 46 rue d'Ulm, 75005 Paris, France;

[2]Laboratoire Colloïdes et Matériaux Divisés, ESPCI, 10 rue Vauquelin, 75005 Paris, France

Author for correspondence:
Pascal J. Lopez
Tel: +33 1 4432 3535
Fax: +33 1 4432 3935
Email: pjlopez@biologie.ens.fr

Received: *13 July 2007*
Accepted: *2 October 2007*

Summary

• Silicon biomineralization is a widespread mechanism found in several kingdoms that concerns both unicellular and multicellular organisms. As a result of genomic and molecular tools, diatoms have emerged as a good model for biomineralization studies and have provided most of the current knowledge on this process. However, the number of techniques available to study its dynamics at the cellular level is still rather limited.
• Here, new probes were developed specifically to label the pre-existing or the newly synthesized silica frustule of several diatoms species.
• It is shown that the LysoTracker Yellow HCK-123, which can be used to visualize silica frustules with common filter sets, presents an enhanced signal-to-noise ratio and allows details of the frustules to be imaged without of the use of ionophores. It is also demonstrated that methoxysilane derivatives can be coupled to fluorescein-5-isothiocyanate (FITC) to preferentially label the silica components of living cells.
• The coupling of labeling procedures might help to address the challenging question of the process of frustule exocytosis.

Key words: 3D-imaging, biomineralization, diatoms, exocytosis, nanopattern.

New Phytologist (2008) **177**: 822–829

doi: 10.1111/j.1469-8137.2007.02303.x

Introduction

Silicon biomineralization is a widespread biological process that concerns a large number of organisms, ranging from animals to higher plants and protists (Epstein, 1999; Ma, 2003; Neumann, 2003; Wilt, 2005; Coradin *et al.*, 2006). In the marine environments, even if this process is found in many different lineages, some major groups dominate: the siliceous sponges, the diatoms, the radiolarians and the silicoflagellates. Interestingly, our current knowledge on the diversity of organisms capable of producing siliceous skeletons is increasing as a result of the discovery of new species (Yoshida *et al.*, 2006) or better phylogeny analyses (Hoppenrath & Leander, 2006). However, diatoms occupy a special place among these organisms because they play major ecological roles in carbon and silicon biochemical cycles (Tréguer *et al.*, 1995; Field *et al.*, 1998; Yool & Tyrrell, 2003).

Diatoms are unicellular eukaryotic algae able to create aesthetic cell walls. They comprise two valves that fit together much like a Petri dish and its lid, and which are made of amorphous silica that present species-specific patterns. Owing to the extensive variety of these natural structures, understanding diatom silicification has recently attracted more attention from chemists, materials scientist and developmental biologists (Coradin & Lopez, 2003; Wilt, 2005). However, studies of diatom cell biology have been hampered in the past by the lack of molecular and cellular tools. This situation is now changing following the emergence of new model species for which the number of molecular tools is increasing (Montsant *et al.*, 2005; Poulsen & Kroger, 2005; Poulsen *et al.*, 2006) and for which full-genome sequences are available (http://genome.jgi-psf.org/Phatr2/Phatr2.home.html; Armbrust *et al.*, 2004). Nevertheless, our understanding of the silica pattern formation remains limited because the description of biomaterials

usually requires high-resolution microscopy techniques that involve cleaning and selection procedures.

So far, very few fluorescent tracers to study silicon biomineralization have been described. For diatoms, because the silica polycondensation process (i.e. frustule formation) occurs during cell division inside an intracellular acidic compartment (a silica deposition vesicle, SDV), acidotropic molecules were shown to accumulate inside the SDV, probably because of the protonation of their side chains, and then become trapped in the newly synthesized silica structures. The pioneer works used rhodamine-123 (Li *et al.*, 1989; Brzezinski & Conley, 1994) as a staining agent, but its low accumulation efficiency limited its use. More recently, the LysoSensor Yellow/Blue DND-160, a useful pH ratiometric indicator (Diwu *et al.*, 1999; Lin *et al.*, 2001), was also used for the imaging of diatom frustules (Shimizu *et al.*, 2001; Hazelaar *et al.*, 2005; Vrieling *et al.*, 2005; Frigeri *et al.*, 2006) and to estimate the Si transport in desmosponges (Schroder *et al.*, 2004).

Here, we establish a novel fluorescent dye, the HCK-123, which is observable in the visible light range and can be used directly to follow the formation of silica structures. Moreover, we also show that fluorescein-5-isothiocyanate (FITC)-silane can be combined with acidotropic probes to distinguish pre-existing or newly synthesized diatom-shell patterns. This latest development is also shown to be useful to monitor the exocytosis of the silica frustule, a process that has hardly been addressed before.

Materials and Methods

Culture and labeling conditions

The cells used are the marine diatoms *Phaeodactylum tricornutum* (clone 1090-1a, Culture Collection of Algae at the University of Göttingen), *Thalassiosira weissflogii* (CCMP 1051, Provasoli-Guillard National Center for Culture of Marine Phytoplankton), *Cylindrotheca fusiformis* (CCMP 343), *Ditylum brightwellii* (CCMP 359), the Prasinophyceae *Prasinococcus* (RCC 520, Roscoff Culture Collection of Marine Phytoplankton), the Coccolithophoridae *Pleurochrysis carterae* clone AC1 and the marine red alga *Rhodella violacea* (strain 115–79, University of Göttingen). The algae were cultured in natural sea water supplemented with Guillard's (F/2) enrichment solution (Sigma) and vitamins. In all cases, cells were cultured at 16°C under a light : dark regime (16 h : 8 h). The yeast and the bacteria were cultured at 30°C in YPD (yeast extract/peptone/dextrose) and at 37°C in Luria broth, respectively.

Silane synthesis

The FITC-silanes were prepared by mixing 0.265 ml of pure (3-amino-propyl)trimethoxysilane (APS) (ABCR GmbH & Co. KG, Karlsruhe, Germany) and 5 μmol of fluorescein isothiocyanate isomer 1 (Sigma-Aldrich, Paris, France) diluted in 5 ml ethanol as a cosolvent (van Blaaderen & Vrij, 1992) and the reaction mixture was stirred at ambient temperature for 2 h. APS was in large excess, with an APS/FITC molar ratio of 200 : 1. Preparations were stable and reactive for a few months, so fresh FITC-APS was made during the different phases of the experiment. Furthermore, to ascertain that the solvent does not have any effect on the cell viability and/or the membrane permeability, the synthesis was performed either in dimethyl sulfoxide (DMSO) or ethanol (EtOH). The results obtained were the same irrespective of the solvent used (data not shown). Alternatively, at the end of these incubations, an excess (0.6 mM final) of hexamethyldisilazane (ABCR) was added to inhibit further polycondensation of the silanes (Haukka & Root, 1994). For overnight or time course experiments, the LysoTrackers (Invitrogen, Cergy Pontoise, France) and FITC-APS were used at 1 μM.

Image acquisition and processing

Images were obtained using a Leica DM-IRB microscope coupled to a Z-stage piezo-controller (Sutter Instrument Company, CA, USA) with a 100 W mercury lamp. The objectives used are ×63 or ×100 (NA 1.4) oil immersion plan APO. The set of filters used for HCK-123 and FITC-APS were 485/25 nm excitation (Ex) and 535/30 nm emission (Em); for DND-160 we used 360/40 nm (Ex) and 535/30 nm (Em), and for the chlorophyll fluorescence signal we used 485/25 nm (Ex) and 675/50 nm (Em). For all these sets the same beam splitter, 86 003 bs (Chroma Technology Corp, Rockingham, VT, USA), was used. The stacks were analyzed using MetaMorph software (Molecular Devices Corporation, CA, USA). All the images presented are 3D reconstructions. However, in some cases, before the reconstruction, a deconvolution step using the Meinel algorithm (Meinel, 1986) and color-specific point spread function was performed.

Frustules purification and transmission electron microscope (TEM) images

Exponentially growing cells were fixed with formaldehyde (final concentration 0.8%) for 1 h at room temperature and then washed several times with distilled water. Organic material was first oxidized by potassium permanganate (final concentration 3%) with an excess of H_2SO_4 and then eliminated with 16% HNO_3 (v/v) and 48% H_2SO_4 (2 : 1, v/v) for 1 min. The suspension was neutralized by adding Tris-HCl buffer (1 M, pH 8), then carefully filtrated and washed with ethanol 95% using a Millipore membrane filter (0.45 μM HV). A drop of the cleaned material was placed on a 300 mesh carbon-coated copper grid and observed with a Philips Tecnai 12 electron microscope.

Results and Discussion

Comparison of the HCK-123 with other lysotrackers

To extend the number of useful probes for imaging the dynamics of the frustule formation, we tested several probes

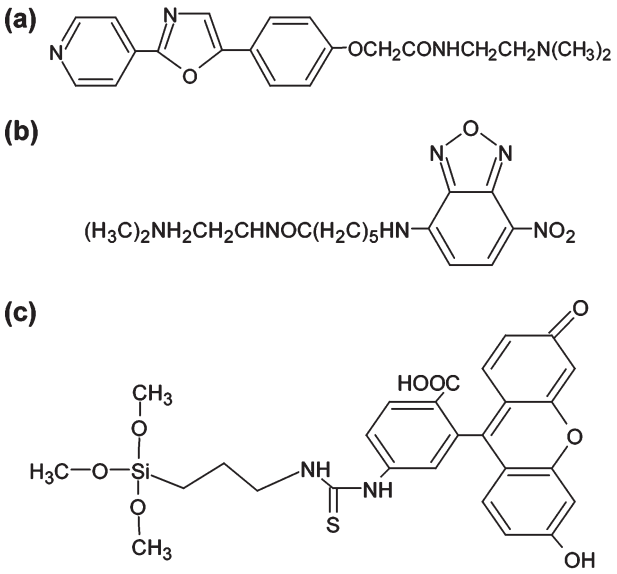

Fig. 1 Chemical structures of the principal dyes used in this work. (a) DND-160 ($C_{20}H_{22}N_4O_3$), also called PDMPO (for 2-(4-pyridyl)-5-((4-(2-dimethylaminoethylamino-carbamoyl)methoxy)phenyl)oxazole); (b) HCK-123 ($C_{16}H_{24}N_6O_4$); (c) fluorescein-5-isothiocyanate (FITC)-silane.

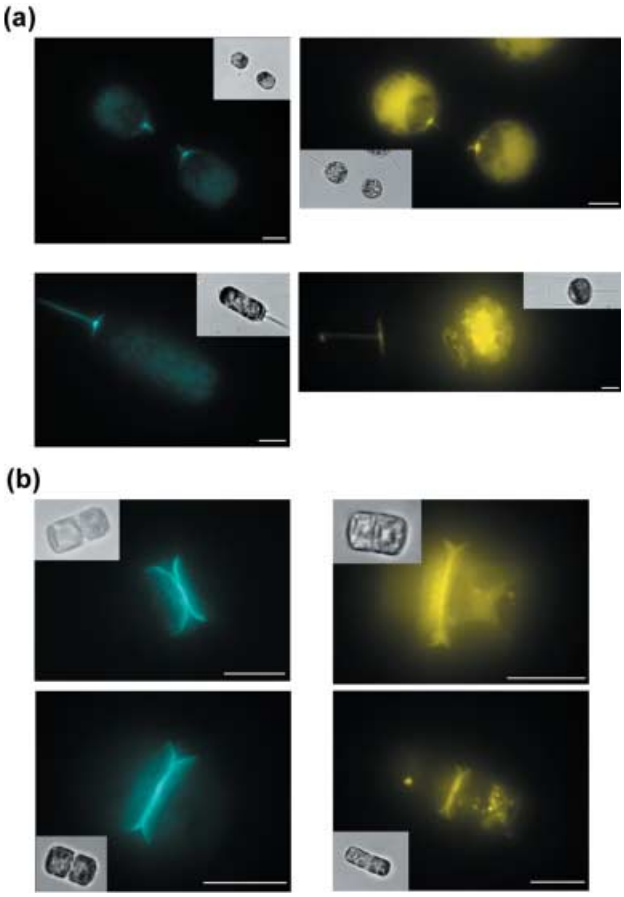

Fig. 2 Comparison of Si-labeling using either HCK-123 or DND-160. (a) *Ditylum brightwellii*; (b) *Thalassiosira weissflogii*. Exponentially growing cells were cultured in the presence of either HCK-123 or DND-160 for approx. 20 h before imaging. Note that the more important 'noise' that corresponds to accumulation of the acidotropic probes is far less important for HCK-123 (yellow, right) than for DND-160 (cyan, left). The maximum signal intensity of each picture was normalized to be about the same value (within 1.5-fold). Bars, 10 μm; insets, bright field images.

for acidic compartments that have different biochemical and fluorescence properties. We found that both the LysoTracker Red DND-99 and the LysoSensor Green DND-153 led to a staining of intracellular membrane components, but extremely weak or no silica labeling, respectively. The LysoSensor Blue DND-167 was thought to be a good tracer because of its high quantum efficiency (Lin *et al.*, 2001), but unfortunately the fluorophore quickly bleaches during light illumination, preventing its use for 3D-imaging. We then tested a membrane-permeable probe, LysoTracker Yellow HCK-123 (Fig. 1a), a weakly basic amine that selectively accumulates in cellular compartments with low luminal pH (i.e. lysosomes; Van Hoof *et al.*, 2002; Burgdorf *et al.*, 2007). For comparison analyses we also used a pyridyl oxazole dye, the LysoSensor Yellow/Blue DND-160 (Fig. 1b). We found that much less background fluorescence was obtained with HCK-123 than with DND-160 for all the diatom species tested. This higher signal-to-noise (S/N) ratio for HCK-123 compared with DND-160 can be easily appreciated by analyses of the signal intensities (Fig. 2a,b). With our settings, the autofluorescence signals were negligible and the intracellular signals corresponded essentially to intravesicular accumulation of the dyes (i.e. accumulation in large vacuoles). However, such a signal can vary according to the species and the physiological state of the cells. For example, for the large *D. brightwellii*, the intracellular DND-160 fluorescence can almost completely mask the newly synthesized frustule (Fig. 2a). For *T. weissflogii*, the dye HCK-123 accumulates almost exclusively in the newly synthesized silica material (Fig. 2b). To increase the S/N ratio it has been recommended to use ionophores (monensin and nigericin, which are polyether ionophores catalyzing K^+ (or Na^+) : H^+ exchanges) (Shimizu *et al.*, 2001); our experiments show that this recommendation does not apply for the Lysoprobe HCK-123. We also found that HCK-123 is more stable, allowing several successive acquisitions, and induces less bleaching of the chloroplast, which suggests that it is less detrimental to cell integrity. Moreover, HCK-123 can be used with common filter sets (e.g. GFP or FITC), allowing it to be used with the vast majority of confocal microscopes that are not equipped with UV excitation.

Altogether, our results prove that different acidotropic pH probes can be used for silica labeling but that their efficiency depends on the ability of the dye to accumulate and to be stable inside acidic compartments. For example, the absence of labeling of DND-153 could be expected since its apparent pKa was measured to be 7.5 (Lin *et al.*, 2001; Molecular

Probes, Invitrogen, Cergy Pontoise, France), therefore limiting its accumulation inside the SDV of diatoms that was estimated to be an acidic compartment (Vrieling *et al.*, 1999). Another criterion for the application of a Lysoprobe for silica labeling might be the stability or the quenching of both the protonated and unprotonated forms upon 'co-precipitation' within the silica materials (see later discussion). Nevertheless, we found that HCK-123 makes a powerful new probe for live cell imaging of the frustule formation.

Sensitivity of the silica labeling

To extend our study of HCK-123 further, we chose important diatom model species for genomic and/or biomineralization studies. To test the sensitivity of the silica labeling, we first investigated two model species that are lightly silicified. We chose the pennate *Cylindrotheca fusiformis*, a well-known species in biochemical studies of organic compounds involved in silica biomineralization (Kroger *et al.*, 2001; Knecht & Wright, 2003; Sumper & Kröger, 2004). For *C. fusiformis* the silica wall is limited to a raphe structure and a large number of girdle bands (Gbs) (Fig. 3a). The raphe is punctuated by rib-like fibulae (their sizes, measured by TEM image analyses, are 102 ± 25 nm; they appear dark in Fig. 3a), which are dense silicified structures separated from one another (by 380 ± 134 nm). With our experimental setup, we could distinguish the nanometric raphe punctuations as well as the more uniform pattern of the Gbs (Fig. 3a). Another species used was *P. tricornutum*, for which genetic manipulation is routine (Lopez *et al.*, 2005) and the full-genome sequence is available. *Phaeodactylum tricornutum* is polymorphic (cells can be fusiform, oval or triradiate) with only the oval morphotype able to synthesize a frustule that is generally unique to one side of the cell (Lewin *et al.*, 1958; Borowitzka & Volcani, 1978). For this latter species, the silica structure labeled with HCK-123 resembles a rib with a denser central nodule and corresponds to the raphe region (Fig. 3b). Finally, we investigated the formation of a single Gb in *T. weissflogii*. For the clone used, the Gbs are split rings with a width of approx. 600 nm. Approximately 1 h following the addition of HCK-123 to exponentially growing cells, we could visualize the formation of a single Gb (Fig. 3c). Altogether our results demonstrate that HCK-123 can be used to follow the formation of reasonably dense silica structures.

Coprecipitation of lysotrackers with newly synthesized frustules

To ascertain that the novel silica tracer, the Yellow HCK-123, was incorporated within the silica matrix *per se*, preparations of biomaterials were made. *Thalassiosira weissflogii* cells were first labeled overnight in the presence of either DND-160 or HCK-123. Since the generation time of the cells was *c.* 12 h, and because labeling was performed overnight, usually only one generation occurred during the labeling period. To purify organic-free silica frustules, cells were first oxidized by potassium permanganate with an excess of H_2SO_4 and then treated with a mixture of strong acids for 1 min (see the 'Materials and

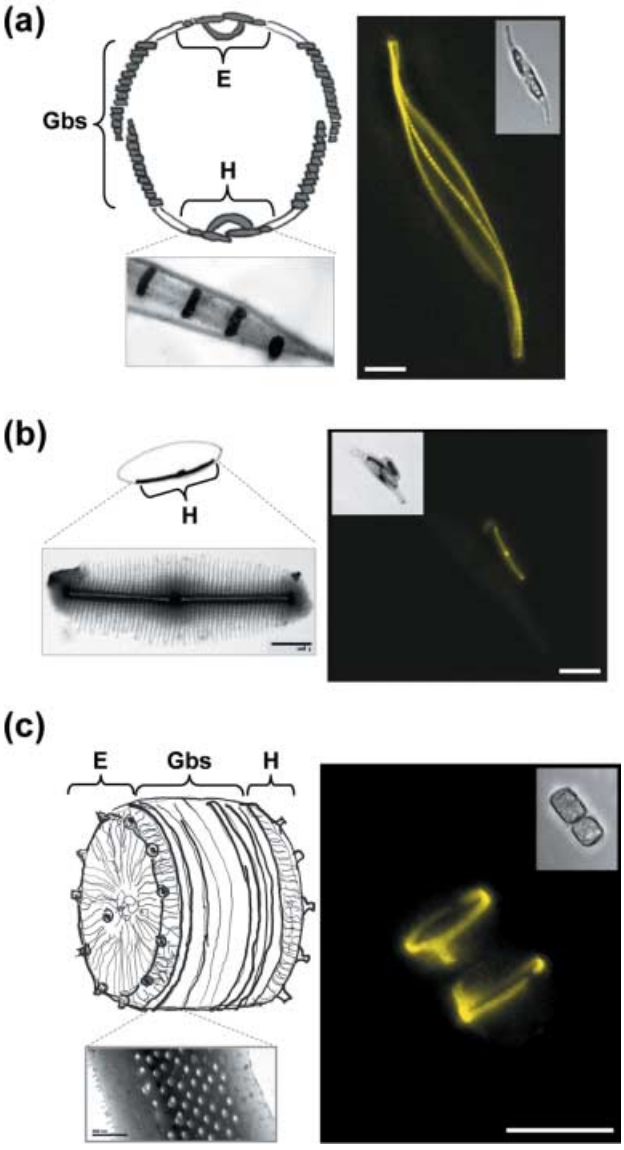

Fig. 3 Sensitivity of HCK-123 labeling. (a) Manual drawing of *Cylindrotheca fusiformis* silica structures. The raphe and the girdle bands (Gbs) are in gray, and the nonsilicified regions are open. The 3D-reconstructed image after staining with HCK-123 (yellow) reveals the nano-patterning of the raphe. (b) Manual drawing of *Phaeodactylum tricornutum* oval cells and transmission electron microscope (TEM) image illustrating the delicate frustule composed of a central raphe with lateral striae. Fluorescent frustules are found only for the oval morphotype. (c) Manual drawing of a complete frustule of *Thalassiosira weissflogii*; the fluorescent image reveals the split rings of two newly divided cells. Note the splits that are nearly 180° apart: the tongue-like sections (ligula). The components of the frustule are the epivalve (E) and the hypovalve (H) that are maintained together by the Gbs. Bars, 5 μm (epifluorescence), 200 nm (TEM).

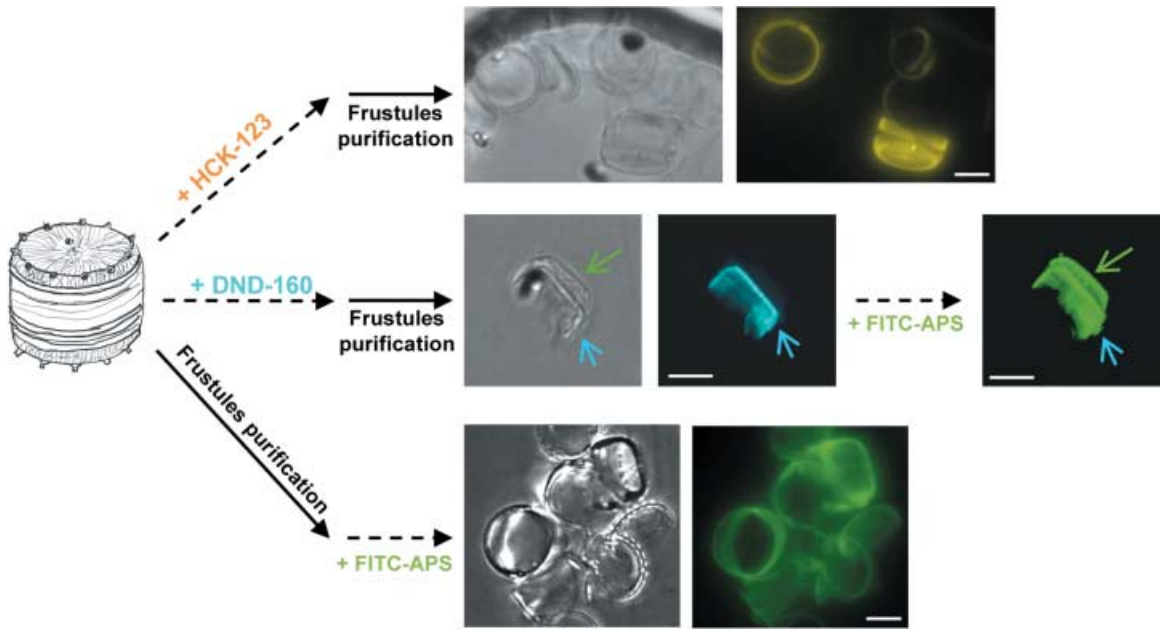

Fig. 4 Strategies followed to label silica frustules. To demonstrate that both DND-160 (cyan) and HCK-123 (yellow) are incorporated and codeposited within newly synthesized silica structures, frustules from overnight cultures were purified. Alternatively, purified frustules could then be stained by incubation with FITC-APS (green). The arrow shows a partial frustule that is revealed only after fluorescein-5-isothiocyanate (FITC) labeling. Bars, 5 μm.

Methods' section). After neutralization, fluorescent images of the purified materials confirmed that both LysoSensors were selectively incorporated and codeposited with Si into newly synthesized frustules (Fig. 4).

In vitro labeling of biogenic silica with FITC-silanes

The need to decipher the silica pattern formation in diatoms has motivated us to explore new kinds of fluorescent dyes that can label the diatom silica structures 'independently' of the underlying intracellular biological processes. Procedures exist to chemically bind a dye molecule to silane coupling agents, which can then be used to coat interior or surface silica particles (van Blaaderen & Vrij, 1992). Such coating involves the formation of Si-O-Si bonds between the surface silanols and the silanes. To the best of our knowledge, the use of silane molecules to label biological samples has seldom been reported (Hodson *et al.*, 1994), but we envisioned that it could be extended to study the silicate structures of living organisms.

The dye FITC was covalently bound to the coupling agent (3-amino-propyl)trimethoxysilane (APS) by an addition reaction of the amine group with the isothiocyanate group. We then performed kinetics studies, with incubation periods varying between 1, 5 and 30 min and up to 16 h, followed by three washing steps to increase the S/N ratio. Because incubation time did not significantly influence the signals, we chose the shortest incubation of 1 or 5 min. As control, silica beads of 1.2 μm prepared from hydrolysis of alkyl silicates and subsequent condensation of silicic acid in alcoholic solutions, as described in Stoëber *et al.* (1968), were labeled with FITC-APS (Fig. 1c). A much weaker signal was obtained when the APS coupling moiety was replaced by (3-aminopropyl) dimethylethoxysilane, which possesses only one reactive alkoxy group coupled to FITC (not shown). These results suggest a coupling of multiple dyes per surface silanol by polycondensation of FITC-APS. Such a hypothesis is in agreement with other studies on the use of alkoxysilanes on precipitated silica (de Monredon *et al.*, 2006). Indeed, it is well established that after hydrolysis, alkoxysilanes can condense, either with the surface silanols (here the ones of the frustule) to produce a monolayer coverage via a siloxane anchoring or with itself, leading to a polysiloxane network on the surface (Osterholtz & Pohl, 1992).

Finally, we checked that organic-free frustules, either untreated or prestained after *in vivo* incorporation of DND-160, could be labeled with FITC-silane (Fig. 4). Altogether these experiments confirmed that FITC-silane can be used specifically to label either synthetic or biogenic silicates *in vitro*.

Use of fluorescent silane to label the silica structure of living organisms

We then carried out a series of similar experiments but with living organisms. We first performed control tests with several species that are not silicified: the bacteria *Escherichia coli*, the baker's yeast *Saccharomyces cerevisiae*, a Prasinophyceae

Prasinococcus, a Coccolithophoridae *Pleurochrysis carterae* and the Rhodophyceae *Rhodella violacea*. Cells cultured in appropriate media were washed before re-suspension in sea water in the presence of FITC-silanes. Except for *R. violacea*, no staining of intra- or extracellular structures was observed, suggesting that the cells are impermeable to this molecule and that the silanes did not interact with organic molecules from the outer membrane or the cell wall components (i.e. glycerophospholipids, lipopolysaccharides (LPS), proteins, glycoproteins and polysacharides). *Rhodella violacea* showed an important intracellular accumulation of the FITC alone or coupled to silane, suggesting that these cells are permeable to the dye molecule (data not shown).

For the diatom *T. weissflogii*, specific fluorescent signals corresponding to the complete frustules were observed after treatment by FITC-silane (Fig. 5a), but no staining was obtained using FITC or fluorescein alone. Similar results were obtained for the other diatoms tested: *C. fusiformis*, *S. costatum* or *D. brightwellii* (not shown). It is worth mentioning that the permeability, and therefore the coating of the biogenic silica, depends on the dye moiety. Indeed, we found for rhodamine-APS a strong intracellular fluorescent signal and a weak staining of the surface (not shown). This result demonstrates that the efficiency of the silane labeling depends on the dye moiety, and can be obtained only if the cells are impermeable to the dye. In addition, careful analyses of the pattern observed for different cells stained with FITC-silane revealed some heterogeneity. For example, we often observed a denser structure in the middle of *T. weissflogii* cells that might correspond to the overlapping region of the Gbs (Figs 5a, 6a). For *T. weissflogii* we also found that one theca was often more fluorescent than the other (Figs 5a, 6a,c). Finally, for *C. fusiformis*, a preferential labeling of the Gbs was reproducibly obtained with the silanes (Fig. 5b). The variations of the labeling might reflect some differences in the accessibility or in the density of the interacting species.

Unfortunately, for *P. tricornutum*, the nonsilicified part of the extracellular matrix was also stained with FITC-silanes, even if this signal was approx. two to threefold weaker than that of the silica frustule (Fig. 5c). However, for the oval cell, asymmetry in the labeling can exist (Fig. 5a, upper panel left). Indeed, the two sides of the cell can be more densely labeled than the middle, suggesting that silanes could interact with some specially localized organic molecules. We also found that the FITC-silane signal was reproducibly weaker in fusiform compared with oval cells (Fig. 5c, upper panel). These results suggest that FITC-APS can interact with some organic-associated materials, but that this interaction depends on the species. To test the specificity of this probe, post-labeled cells were treated with the anionic surfactant sodium dodecyl sulfate (which is commonly used to destabilize electrostatic interactions). After treatment for 5 min in 2% SDS, 100 mM EDTA at 95°C, the *T. weissflogii* frustule was still stained, although with a slightly reduced signal (Fig. 5a); for *P. tricornutum*, only the frustule-associated fluorescence remained, whereas organic matrix labeling disappeared (Fig. 5c, upper and lower panels). The specificity of the frustule-associated staining was also confirmed for the other kinds of diatom tested. We interpret that after hydrolysis of the three methanol moieties, which will occur in aqueous environments, amino-propyl silanes form stable Si-O-Si bridges with accessible surface silanols, leading to stable and resistant staining. Altogether our results demonstrate that FITC-APS can be used to visualize

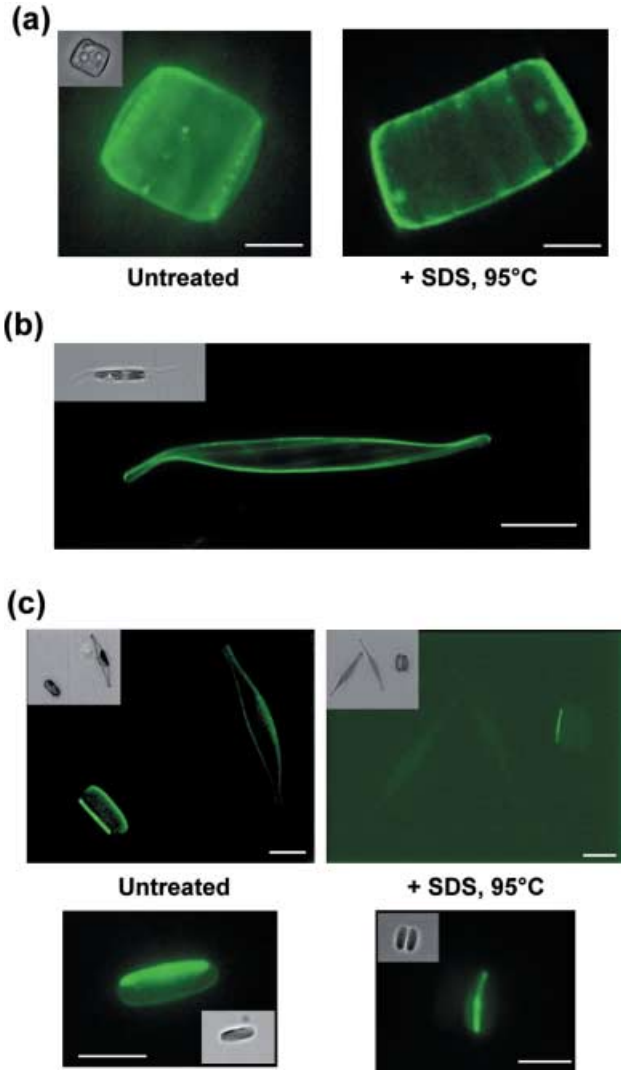

Fig. 5 Labeling of diatom-silica with fluorescein-5-isothiocyanate (FITC)-silane. Living cells were treated with FITC-APS for 1 min and then washed before image acquisition. (a) *Thalassiosira weissflogii*: the complete frustule is stained and the labeling is essentially the same after treatment in SDS/EDTA for 5 min at 95°C. (b) *Cylindrotheca fusiformis*: the labeling corresponds mainly to the Gbs region. (c) *Phaeodactylum tricornutum*: the preferential labeling with FITC-APS that appears as a rib-like structure corresponds to the frustule. However, even if fusiform cells also present a labeling, only the silica frustule remains fluorescent after SDS/EDTA treatment. Also note the asymmetric staining of the organic part in some oval cells (lower panel). Insets, bright filed images. Bars, 5 μm.

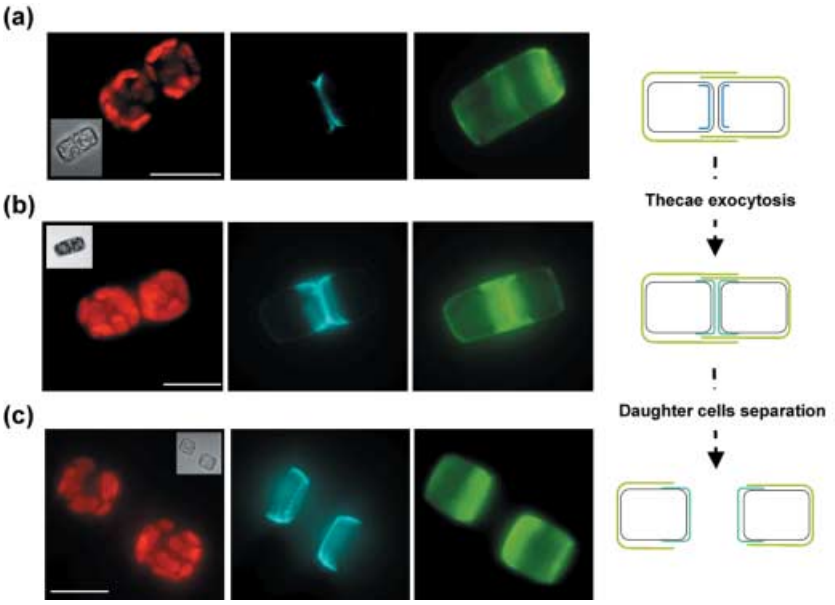

Fig. 6 Frustule accessibility can be studied by dual labeling. *Thalassiosira weissflogii* cells were grown in the presence of DND-160 (cyan) and then labeled with fluorescein-5-isothiocyanate (FITC)-silanes (green). (a) Before exocytosis, the hypothecae newly synthesized within the two daughter cells are stained only by DND-160. (b) After silica deposition vesicle (SDV) exocytosis, the new hypothecae present a dual labeling with both DND-160 and FITC-silanes. Later, the daughter cells will separate and the newly formed silica material is clearly visible (c). Insets correspond to bright fields, and red images to chlorophyll fluorescence.

the part of the frustules that is accessible from the external environment.

Combination of dyes can help to study the release of the frustule

We believed that the combination of different probes – that is, Lysotrackers that stain newly synthesized structures and FITC-silane that has access only to extracellular materials – could be used to address the secretion of the valve and Gbs, something that has never before been possible. For this purpose, exponentially growing cells were incubated with DND-160 and then with FITC-APS. For these experiments we found that DND-160 was a very useful dye since its excitation does not overlap in wavelength with FITC-silane. However, we are currently testing new fluorescent silanes (e.g. Texas red, Alexa Fluor) that can be used in combination with the powerful HCK-123. As illustrated in Fig. 6, we found that, in some *T. weissflogii* cells, the newly synthesized valves are stained only with DND-160 (Fig. 6a); but more frequently in dividing cells the new hypovalves were labeled with both the DND-160 and FITC-silanes (Fig. 6b). After the daughter cells' separation, the dual labeling of the newly synthesized hypothecae is even more visible (Fig. 6c). A likely explanation is that, as we have shown that FITC-silanes do not accumulate inside the cells, the newly synthesized material which is still inside the SDV is not accessible to FITC-silanes. Upon release, this new silica material becomes stained by the FITC-silanes. Even if at this stage we could not perform a similar experiment using the coupled HCK-123 and rhodamin-silane (see earlier discussion), these experiments suggest that coupling of a lysoprobe with a fluorescent-silane could be very useful in studying the accessibility of the silica material.

Conclusions

The present study provides novel procedures to analyze the silica structure of living cells with the help of fluorescent markers. We have developed the use of a new probe, the LysoTracker Yellow HCK-123, which can be used to follow the silica formation process *in vivo*. HCK-123 shows an enhanced S/N ratio and should make a better live probe since it is excitable in the visible range (i.e. less detrimental for the cell viability). In addition, it opens the possibility of using several fluorescent LysoProbes to study mixed populations or perform combined pulse-chase experiments. In addition, we have started the development of another rapid procedure to analyze the pattern of diatom shells by using FITC-silane coupling agents. In future, since a large number of other amine reactive fluorescent dyes can be coupled to APS, we believe that a full panel of fluorescent-silanes could be exploited to address the questions of diatom pattern formation *in vivo*. Further studies using combinations of different kinds of molecular properties and specificities should help to address the localization and accessibility of diatom frustules, and hopefully explore the process of frustule exocytosis. Such strategies might also be used to screen for drugs that specifically inhibit the release of the frustule but not its formation. The aforementioned approaches may also be of interest in the study of silicon biomineralization in other unicellular or multicellular organisms.

Acknowledgements

We thank I. Probert and C. De Vargas for providing the strain *Pleurochrysis carterae*, and D. Vaulot and F. Le Gall for providing *Prasinococcus*. Research in P. J. L. laboratory is supported in

part by the Marine Genomics Europe Network. J.D. and G.S. were fellows from the European STREP Diatomics (LSHG-CT-2004-512035).

References

Armbrust EV, Berges JA, Bowler C, Green BR, Martinez D, Putnam NH, Zhou S, Allen AE, Apt KE, Bechner M *et al.* 2004. The genome of the diatom *Thalassiosira pseudonana*: ecology, evolution, and metabolism. *Science* **306**: 79–86.

van Blaaderen A, Vrij A. 1992. Synthesis and characterisation of colloidal dispersions of fluorescent, monodisperse silica spheres. *Langmuir* **8**: 2921–2931.

Borowitzka MA, Volcani BE. 1978. The polymorphic diatom *Phaeodactylum tricornutum*: ultrastructure of its morphotypes. *Journal of Phycology* **14**: 10–21.

Brzezinski MA, Conley DJ. 1994. Silicon deposition during the cell cycle of *Thalassiosira weissflogii* (Bacillariophyceae) determined using dual rhodamine 123 and propidium iodide staining. *Journal of Phycology* **30**: 45–55.

Burgdorf S, Kautz A, Bohnert V, Knolle PA, Kurts C. 2007. Distinct pathways of antigen uptake and intracellular routing in cd4 and cd8 t cell activation. *Science* **316**: 612–616.

Coradin T, Desclés J, Luo G-Z, Lopez PJ. 2006. Silicon in the photosynthetic lineages: molecular mechanisms for uptake and deposition. In: Teixeira da Silva JA, ed. *Floriculture, ornamental and plant biotechnology: advances and topical issues*. London, UK: Global Science Books, 101–107.

Coradin T, Lopez PJ. 2003. Biogenic silica patterning: simple chemistry or subtle biology? *ChemBioChem* **4**: 251–259.

Diwu Z, Chen CS, Zhang C, Klaubert DH, Haugland RP. 1999. A novel acidotropic pH indicator and its potential application in labeling acidic organelles of live cells. *Chemistry & Biology* **6**: 411–418.

Epstein E. 1999. Silicon. *Annual Review Plant Physiology and Plant Molecular Biology* **50**: 641–664.

Field CB, Behrenfeld MJ, Randerson JT, Falkowski P. 1998. Primary production of the biosphere: integrating terrestrial and oceanic components. *Science* **281**: 237–240.

Frigeri LG, Radabaugh TR, Haynes PA, Hildebrand M. 2006. Identification of proteins from a cell wall fraction of the diatom *Thalassiosira pseudonana*: insights into silica structure formation. *Molecular & Cellular Proteomics* **5**: 182–193.

Haukka S, Root A. 1994. The reaction of hexamethyldisilazane and subsequent oxidation of trimethylsilyl groups on silica studied by solid-state NMR and FTIR. *Journal of Physical Chemistry* **98**: 1695–1703.

Hazelaar S, van der Strate HJ, Gieskes WWC, Vrieling EG. 2005. Monitoring rapid valve formation in the pennate diatom *Navicula salinarum* (Bacillariophyceae). *Journal of Phycology* **41**: 354–358.

Hodson MJ, Smith RJ, van Blaaderen A, Crafton T, O'Neill CH. 1994. Detecting plant silica fibres in animal tissue by confocal fluorescence microscopy. *The Annals of Occupational Hygiene* **38**: 149–160.

Hoppenrath M, Leander BS. 2006. Ebriid phylogeny and the expansion of the cercozoa. *Protist* **157**: 279–290.

Knecht MR, Wright DW. 2003. Functional analysis of the biomimetic silica precipitating activity of the R5 peptide from *Cylindrotheca fusiformis*. *Chemical Communicatios* **24**: 3038–3039.

Kroger N, Deutzmann R, Sumper M. 2001. Silica-precipitating peptides from diatoms. The chemical structure of silaffin-a from *Cylindrotheca fusiformis*. *The Journal of Biological Chemistry* **276**: 26066–26070.

Lewin JC, Lewin RA, Philpott DE. 1958. Observations on *phaeodactylum tricornutum*. *Journal of General Microbiology* **18**: 418–426.

Li C-W, Chu S, Lee M. 1989. Characterizing the silica deposition vesicle of diatoms. *Protoplasma* **151**: 158–163.

Lin HJ, Herman P, Kang JS, Lakowicz JR. 2001. Fluorescence lifetime characterization of novel low-pH probes. *Analytical Biochemistry* **294**: 118–125.

Lopez PJ, Descles J, Allen AE, Bowler C. 2005. Prospects in diatom research. *Current Opinion in Biotechnology* **16**: 180–186.

Ma JF. 2003. Functions of silicon in higher plants. *Progress in Molecular Subcellular Biology* **33**: 127–147.

Meinel ES. 1986. Origins of linear and nonlinear recursive restoration algorithms. *Journal of Optical Society of America A* **3**: 787–799.

de Monredon S, Pottier A, Maquet J, Babonneau F, Sanchez C. 2006. Characterisation of the grafting of (3-aminoethyl)amino-propyltrimethoxysilane on precipitated silica. *New Journal of Chemistry* **30**: 797–802.

Montsant A, Maheswari U, Bowler C, Lopez PJ. 2005. Diatomics: toward diatom functional genomics. *Journal of Nanoscience and Nanotechnology* **5**: 5–14.

Neumann D. 2003. Silicon in plants. *Progress in Molecular Subcellular Biology* **33**: 149–160.

Osterholtz FD, Pohl ER. 1992. Kinetics of the hydrolysis and condensation of organofunctional alkoxysilanes: a review. *Journal of Adhesive Science and Technology* **6**: 127–149.

Poulsen N, Chesley PM, Kroger N. 2006. Molecular genetic manipulation of the diatom *Thalassiosira pseudonana* (Bacillariophyceae). *Journal of Phycology* **42**: 1059–1065.

Poulsen N, Kroger N. 2005. A new molecular tool for transgenic diatoms. *The FEBS Journal* **272**: 3413–3423.

Schroder HC, Perovic-Ottstadt S, Rothenberger M, Wiens M, Schwertner H, Batel R, Korzhev M, Muller IM, Muller WE. 2004. Silica transport in the demosponge *suberites* domuncula: fluorescence emission analysis using the PDMPO probe and cloning of a potential transporter. *The Biochemical Journal* **381**: 665–673.

Shimizu K, Del Amo Y, Brzezinski MA, Stucky GD, Morse DE. 2001. A novel fluorescent silica tracer for biological silicification studies. *Chemistry & Biology* **8**: 1051–1060.

Stoëber W, Fink A, Bohn E. 1968. Controlled growth of monodispersed silica spheres in the micron size range. *Journal of Colloid and Interface Science* **26**: 62–69.

Sumper M, Kröger N. 2004. Silica formation in diatoms: the function of long-chain polyamines and silaffins. *Journal of Materials Chemistry* **14**: 2059–2065.

Tréguer P, Nelson DM, Van Bennekom AJ, DeMaster DJ, Leynaert A, Quéguiner B. 1995. The silica balance in the world ocean: a re-estimate. *Science* **268**: 375–379.

Van Hoof D, Rodenburg KW, Van der Horst DJ. 2002. Insect lipoprotein follows a transferrin-like recycling pathway that is mediated by the insect LDL receptor homologue. *Journal of Cell Science* **115**: 4001–4012.

Vrieling EG, Gieskes WWC, Beelen TPM. 1999. Silicon deposition in diatoms: control by the pH inside the silicon deposition vesicle. *Journal of Phycology* **35**: 548–559.

Vrieling EG, Sun Q, Beelen TP, Hazelaar S, Gieskes WW, van Santen RA, Sommerdijk NA. 2005. Controlled silica synthesis inspired by diatom silicon biomineralization. *Journal of Nanoscience and Nanotechnology* **5**: 68–78.

Wilt FH. 2005. Developmental biology meets materials science: morphogenesis of biomineralized structures. *Developmental Biology* **280**: 15–25.

Yool A, Tyrrell T. 2003. Role of diatoms in regulating the ocean's silicon cycle. *Global Biogeochemical Cycles* **17**: 103.

Yoshida M, Noel MH, Nakayama T, Naganuma T, Inouye I. 2006. A haptophyte bearing siliceous scales: ultrastructure and phylogenetic position of *Hyalolithus neolepis* gen. et sp. Nov. (Prymnesiophyceae, Haptophyta). *Protist* **157**: 213–234.

